GDCh
Research Article
Angewandte International Edition Chemie
www.angewandte.org

How to cite: Angew. Chem. Int. Ed. **2025**, e202424776
doi.org/10.1002/anie.202424776

Endohedral Fullerenes *Hot Paper*

Inverse Electron Demand Diels–Alder Reaction on $M_3N@C_{80}$ (M = Lu, Sc): Reactivity and Reversibility Enable Chemical Separation of Metallofullerenes

Yue Sun, Laura Abella, Thomas J. Emge, Sheng Zhu, Yanbang Li, Ian Ferraro, Anyin Li, Steven Stevenson, Josep M. Poblet, Antonio Rodríguez-Fortea, and Jianyuan Zhang**

Abstract: Endohedral metallofullerenes are chemically more inert compared to empty fullerenes, primarily due to their intramolecular electron transfer. In this work, we report an inverse electron demand Diels–Alder (IEDDA) reaction on $M_3N@C_{80}$ (M = Lu, Sc), where they show significantly higher reactivity than empty fullerenes. The molecular structures of the [4+2] cycloadducts were unambiguously characterized. Moreover, the cycloadducts can fully revert to pristine $M_3N@C_{80}$ via retro-cycloaddition upon thermal treatment. With the unusual reactivity and reversibility, the IEDDA reaction enables an effective separation approach for metallofullerenes from their soot extracts, opening path to efficient and economical scale-up synthesis of metallofullerenes in laboratory and industrial settings.

Introduction

Endohedral metallofullerenes (EMFs) provide a versatile molecular platform for modulating the properties of encapsulated metals.[1–4] Over the past two decades, EMFs have been extensively studied across various research fields, such as biomedicines,[5–7] single-molecule magnets (SMMs)[8–12] and quantum information sciences.[13–16] To realize these great promises as a family of functional materials, it is critical for EMFs to achieve both high production yields (material availability) and efficient functionalization reactions (tailoring and processing). However, these two desired features are in an inherent conflict: higher yields are associated with more stable structures, which typically indicate chemical inertness. As a classical instance, among all EMFs, $M_3N@I_h\text{-}C_{80}$ exhibit highest production yields due to their high symmetry and stability.[17–19] Meanwhile, they tend to be considerably more inert compared to empty fullerenes and conventional metallofullerenes; in other words, more difficult to functionalize.

Indeed, only a limited number of reactions reported for empty fullerenes have been successfully adapted for EMFs, especially the $M_3N@I_h\text{-}C_{80}$ species, where lower reactivities are consistently observed, including photochemical reactions,[20–22] Diels–Alder (DA) reactions,[23–26] Prato reactions,[27,28] Bingel-Hirsch reactions[29,30] and radical addition reactions.[31,32] The fundamental challenge in their functionalization is their high-lying LUMO making them inefficient electron acceptors.

In a paradigm shift, we herein report a new EMF reaction in which $M_3N@I_h\text{-}C_{80}$ (M = Lu, Sc) act as electron donors and benefit from their high-lying MOs (Figure 1a). In our design, instead of common dienes, diimines react as the electron acceptors with $M_3N@I_h\text{-}C_{80}$ (shortened as $M_3N@C_{80}$ thereafter) as opposed to donors, in an inverse electron demand Diels–Alder (IEDDA) reaction.[33,34] The inverse direction of electron transfer is dictated by the better match of the LUMO of the diimines and the HOMO of the EMFs (Figure 1b). In these reactions, the EMFs showed remarkably higher reactivity than empty fullerenes,[35] resulting in [5,6]-closed products which were characterized by HPLC, MS, UV/Vis, NMR spectroscopy and X-ray diffraction analysis (Figure 2a). Cationic $[Li@C_{60}]^+$ has also been shown to have much higher reactivity than C_{60} in Diels–Alder reactions,[36,37] diazo additions,[38] and [2+2] cycloadditions[39] due to the encapsulated Lewis acid. Our work trailblazes a new approach that exploits the electron-rich nature of neutral EMFs to achieve greater reactivity than empty fullerenes, demonstrated through a direct comparison, in an inverse-electron-demand cycloaddition. Remarkably, both Lu and Sc EMF adducts can undergo

---

[*] Dr. Y. Sun, Dr. T. J. Emge, S. Zhu, Dr. Y. Li, Prof. J. Zhang
Department of Chemistry and Chemical Biology,
Rutgers, The State University of New Jersey,
123 Bevier Rd, Piscataway, NJ 08854 (USA)
E-mail: jy.zhang@rutgers.edu

Dr. L. Abella, Prof. J. M. Poblet, Prof. A. Rodríguez-Fortea
Departament de Química Física i Inorgànica,
Universitat Rovira i Virgili,
Marcel·lí Domingo 1, 43007 Tarragona (Spain)
E-mail: antonio.rodriguezf@urv.cat

I. Ferraro, Prof. A. Li
Department of Chemistry, University of New Hampshire,
23 Academic Way, Durham, NH, 03824 (USA)

Prof. S. Stevenson
Department of Chemistry and Biochemistry and FIRST Molecules Center, Purdue University Fort Wayne, Fort Wayne, IN 46805 (USA)

complete retro-cycloaddition back to pristine EMFs upon heating.

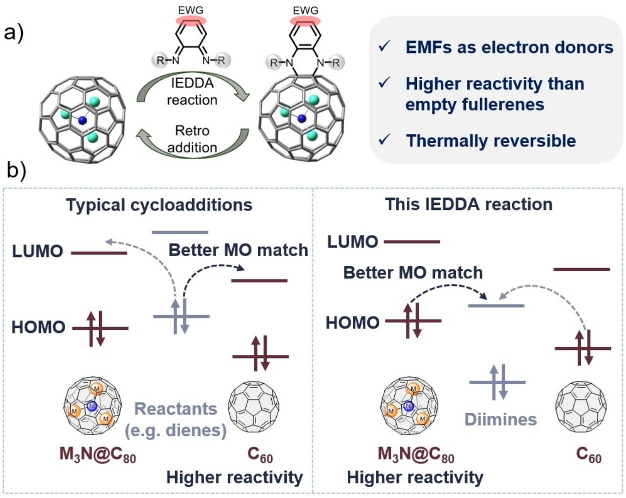

Figure 1. a) The IEDDA reaction Scheme. b) The MO diagrams of fullerenes/EMFs in typical cycloadditions (left) and the IEDDA reaction (right).

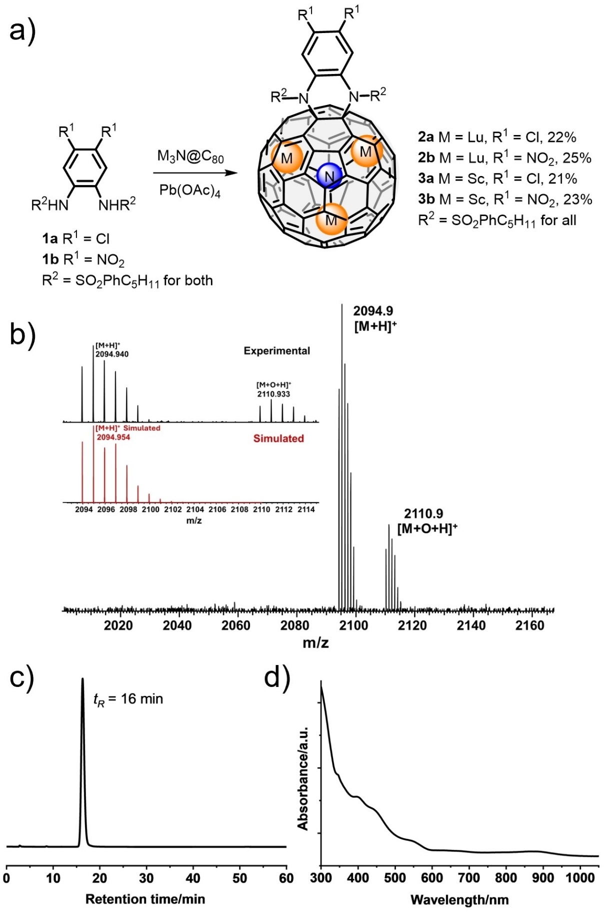

Figure 2. a) Preparation of [4+2] adducts. b) ESI-MS spectrum of **2a**. c) HPLC trace of **2a** (5-PYE, toluene, 2 ml/min). d) UV/Vis absorption spectrum of **2a** in toluene.

The higher reativity (by design) and the full reversibility (unexpected) allowed us to develop a powerful non-chromagraphic strategy to isolate EMFs in scale-up syntheses. The EMFs can be "fished out" by the IEDDA reaction at room temperature and regenerated by thermal treatment. This novel strategy is far more economical and environmetal-friendly than existing organic chemical separations because it only needs chemicals to react with a small portion (the EMFs) rather than the majority (empty fullerenes) of components in the soot, while empty fullerenes are intact and can still be used for other applications.

Results and Discussion

Reaction and Characterization of Products

In DA reactions, fullerenes generally act as good dienophiles owing to their electron-deficient character.[40–42] There have been few studies on the IEDDA reaction on fullerenes, due to the electron-accepting nature of both fullerenes and dienes, which tend to require harsh conditions[43,44] or additional supramolecular strategies.[45]

In this work, the quinone diimine intermediates generated from the in situ oxidation of protected *o*-phenylenediamines[46] react with the double bonds on the fullerene cages to form cycloadducts. The IEDDA reaction mechanism has been established on empty fullerenes,[35] yielding [6,6]-adducts from C_{60} and a *dd*-[5,6] adduct as the major product from C_{70}, respectively (Figure S1). In the current work, reactions were performed on electron-withdrawing group (EWG), -Cl or -NO_2, substituted disulfonamides (**1a**, **1b**) and $M_3N@C_{80}$ (M = Lu, Sc), respectively, in presence of $Pb(OAc)_4$ as the oxidant (Figure 2a). In addition to R^1, the strong EWG, -$SO_2PhC_5H_{11}$, was also used to further bestow electron deficiency of the diamine, and meanwhile, higher solubility of the product. This design is in direct contrast with common DA reactions, where electron-donating groups are preferred.[24] The reactions of **1a** were conducted with heating at 80 °C in *o*-dichlorobenzene (*o*-DCB) for 3 h. With stronger EWGs, i.e., -NO_2, the reactions of **1b** underwent at room temperature.

Four EMF derivatives **2a**, **2b**, **3a**, and **3b** were purified by flash chromatography and fully characterized by HPLC, ESI-MS, UV/Vis, NMR spectroscopy, and finally, single-crystal X-ray crystallography (Figures S2–22, Tables S1–14). The molecular ion peak in the ESI-MS spectrum (Figure 2b, S5) matches the mass of the expected [4+2] cycloadduct. Although in the reaction mixture, as well as the purified product right from the column, the HPLC peak (5-PYE) of the product showed asymmetry, upon leaving the products in solution at room temperature, the peaks merged into a sharp, symmetric peak without any purification (Figure 2c, S4, S13, S16, S19), which indicates its regioisomeric purity. The samples that correspond to the single HPLC peak were used in all further characterizations, including UV/Vis, NMR, and crystallography. The peak assymetry could be due to the temporary existance of another isomer, or the coexistence of multiple conformations of the same compound (see detailed discussion below). The UV/Vis spectrum of **2a** (Figure 2d) shows four weak absorptions centered at 401, 446, 552, and 875 nm, respectively, among which the single peak above 600 nm is consistent with reported [5,6]-adducts.[28,47]

Finally, the structures of **2a** and **3a** were determined by X-ray diffraction analysis, which confirmed the [5,6]-closed structures (Figure 3). The rotational disorder of both pentyl phenyl groups at the extrema of **2a** are modeled as two parts, with ratios of 60:40 for both groups (Figure S22). More notably, the disorder in the position of the Lu_3N cluster is modeled as two separate components with different orientations, occupancies of 84 % and 12 %, and very similar geometries that were subsequently restrained to have similar interatomic geometries during refinement. Both models of the Lu_3N disorder show that two Lu atoms have the Lu-N-Lu bisector directed towards the C–C addition bridge, and the most disordered third Lu atom is directed away from the addend. The Lu-N–Lu bond angles of the major occupancy are 117.0°, 121.1°, and 121.3°, respectively, adding up to 359.4° (same for the minor occupancy), confirming the planarity of the Lu_3N cluster is retained after the cycloaddition. The orientation of the Sc_3N cluster in **3a** (Figure S22) is essentially the same as that of the Lu_3N in **2a**, with the most disordered metal site directed away from the adduct bridge and a planar cluster, which are shared characteristics of many [5,6]-closed adducts of $M_3N@C_{80}$.[24,27,48–50]

DFT computations show that the [5,6]-adduct is the thermodynamically favored product in the reaction for $Lu_3N@C_{80}$. Different conformations of [5,6]- and [6,6]-adducts were computed, revealing that the [6,6]-adduct is 14.4 kcal·mol^{-1} higher in energy (Figure S23). In terms of Gibbs free energy, the [5,6]-adduct of **2a** was confirmed to be the thermodynamic product at 80 °C (Figure S24). Moreover, the Gibbs free energy profiles of $Lu_3N@C_{80}$ and C_{60} show that the experimental products are also the kinetic products (Figure S25).

The regioselectivity is also supported by the frontier molecular orbital (FMO) theory. In this IEDDA reaction, the LUMO of the diimine interacts with the HOMO of the fullerene (Figure 1). Inspecting the orbital shape and distribution of the HOMO of $M_3N@C_{80}$, it is clear that orbital coefficients on C atoms of [5,6] bonds are significantly larger than those of [6,6] bonds (Figure S26). The FMO theory is also powerful to explain the unusual regioselectivity in the reaction of C_{70},[35] where the *dd*-[5,6] adduct was found as the major product.

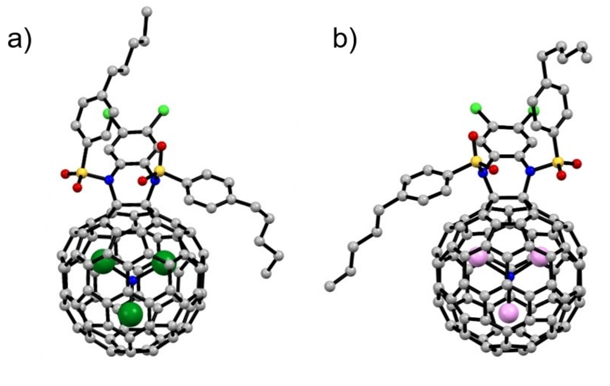

Figure 3. Single-crystal X-ray crystallographic structure of a) **2a**; b) **3a**. Minor sites due to disorder of addends are omitted for clarity.

With the addition of a symmetrical group on the [5,6] bond, a horizontal plane of symmetry is introduced, which could be reflected in the NMR spectra.[27] However, in the ^1H NMR spectrum of **2a** (Figure 4a), two sets of peaks with a ratio of 1:1.2 were observed, indicating the asymmetrical structure of the added group. The ^{13}C NMR spectrum of **2a**, whose peaks were partially assigned based on additional 1D and 2D NMR spectra (Figure S7–S12), also shows two distinct peaks of the two sp^3 addition sites at 80.9 and 81.4 ppm indicating asymmetry (Figure 4b). Without the unambiguous single-crystal elucidation, one might have deduced the products as [6,6] isomers based on the breaking of symmetry.[27,28] However, with single-crystal results confirming the [5,6] addition, we hypothesize that **2a** has two coexisting conformations, as a result of hindered inversion of the two N atoms attached to the cage and tetrahydroquinoxaline ring conformation.

To verify our hypothesis, a computational study was done on the optimized configurations of **2a**, which include

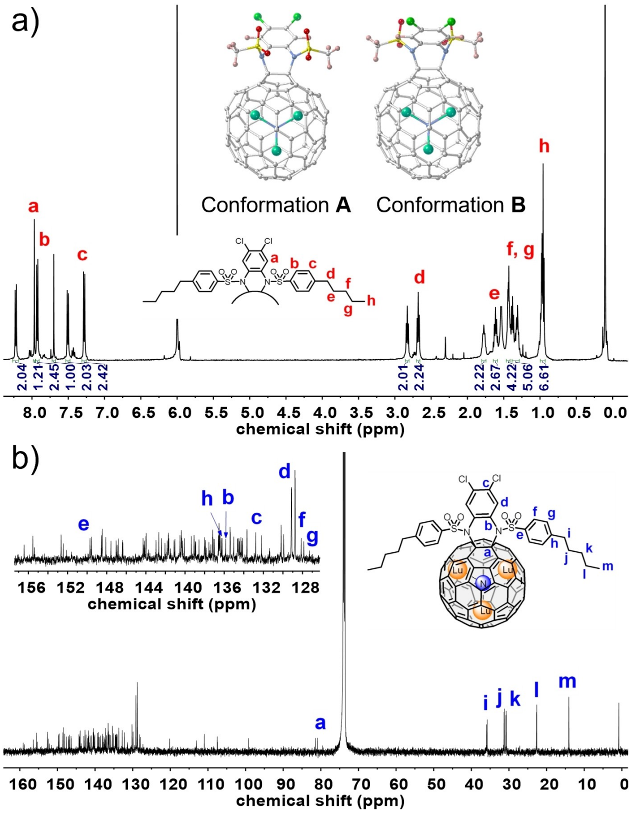

Figure 4. a) ^1H NMR spectrum (500 MHz, $CS_2/CDCl_2CDCl_2$, 25 °C) of **2a** (Inset: two conformations of the model system of **2a**), proton assignment in one conformation is labeled in red. b) ^{13}C NMR spectrum (126 MHz, $CS_2/CDCl_2CDCl_2$, 25 °C) of **2a**, partial carbon assignment is labeled in blue.

different orientations of both the added group and inner metal cluster (Figure S27). Indeed, two conformations, **A** and **B**, are found to have the lowest and same energy (Figure 4a inset). These two conformations correspond to the sulfonyl substituents on the nitrogen atom pointing towards either the pentagon or the hexagon of the [5,6] junction. In most cases, these conformations should interconvert rapidly; however, the NMR results suggest that such interconversion is slower than the NMR timescale due to sterically restricted nitrogen inversion. Therefore, two sets of peaks, instead of one averaged result, were observed in the NMR spectra.

To further validate the presence of interconverting conformation **A** and **B** from the same isomer, variable-temperature (VT) ^{1}H NMR experiments were performed on **2a** from 253 K to 333 K (Figure 5), and then in a reverse ramp back to 253 K (Figure S28). The integral ratio between the two characteristic methylene peaks (highlighted in Figure 5) was tracked to reveal the ratio between conformations **A** and **B**. The **A**/**B** ratio decreased from 1.37 at 253 K to 1.19 at 333 K, with rising temperature, and the trend was reversed with decreasing temperature (Figure S28). This reversible redistribution between **A** and **B** species is consistent with our hypothesis of slowly interconverting conformers that are almost identical in energy (see Supporting Information Discussion).

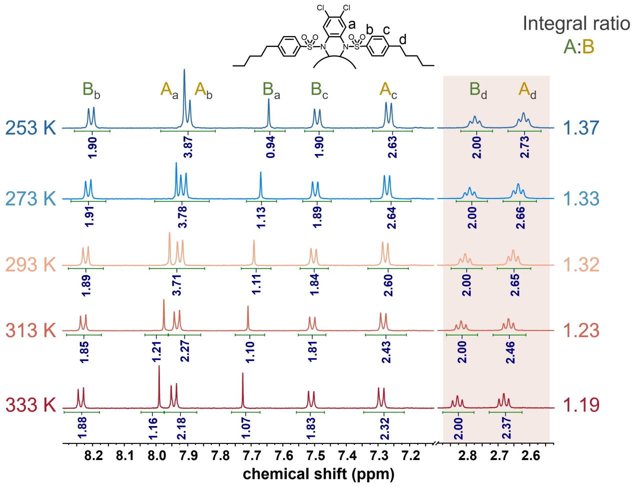

Figure 5. VT ^{1}H NMR spectra of **2a** ranging from 253 to 333 K.

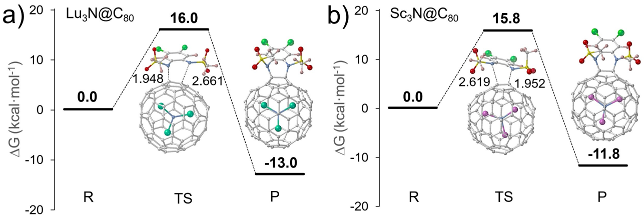

Figure 6. a) Gibbs free energy profiles of the reactions at 80 °C in *o*-DCB for $Lu_3N@C_{80}$ and b) $Sc_3N@C_{80}$. The C–N distances (in Å) between the fullerene and the diimine in the transition states are plotted.

Reactivity Comparison

The reaction pathways were modeled by DFT computation to understand the reactivity of the EMFs. A concerted mechanism going through an asymmetric transition state is the more favorable pathway (Figure 6a, b). With that said, a stepwise mechanism[51] cannot be excluded, as the modeling of the $Lu_3N@C_{80}$ reaction showed that a singly-bonded intermediate is only slightly higher in free energy by 1.9 kcal mol^{-1} (Figure S29). In the concerted cycloaddition, 80 °C in *o*-DCB, the free-energy barrier ($\Delta G^{\neq}$) of $Sc_3N@C_{80}$ is 0.2 kcal mol^{-1} lower than that of $Lu_3N@C_{80}$ (15.8 *vs* 16.0 kcal mol^{-1}) suggesting very similar reactivity between $Lu_3N@C_{80}$ and $Sc_3N@C_{80}$ (Figure 6a, b). Indeed, such subtle difference in activation energy was not observed at our reaction temperature that formed **2a** and **3a**. The slightly higher reactivity of $Lu_3N@C_{80}$ was only experimentally observed at 35 °C (with lower reaction rate and conversion) in HPLC tracking of the reactions (Figure S30, S31). This result contrasts precedents that $Sc_3N@C_{80}$ showed lower reactivity than $Lu_3N@C_{80}$,[22,52] but is consistent with the new role of EMFs as electron donors in IEDDA reactions.

More importantly, in the IEDDA reaction, $M_3N@C_{80}$ are expected to show higher reactivity than empty fullerenes that is attributed to the more electron-rich carbon cages. The observation of a much milder reaction condition for $M_3N@C_{80}$ than C_{60} and C_{70} in the reactions with **1b** with strong EWG $-NO_2$, i.e., room temperature for EMFs *vs* 80 °C for empty fullerenes, indicates the substantially higher reactivity of the two EMFs.

For a direct comparison, a mixture of C_{60}, C_{70} and $Lu_3N@C_{80}$ (10/12/1 mass ratio) in *o*-DCB was prepared, to which small amounts of **1b** and $Pb(OAc)_4$ were added to run a competitive reaction. The components in solution were monitored by HPLC. After stirring at room temperature for 30 min, the peak of $Lu_3N@C_{80}$ dramatically decreased while the peaks of empty fullerenes remained nearly unchanged (Figure 7). Independent studies confirmed that C_{60} and C_{70} do not react with **1b** at room temperature (heating was required).35 The direct comparison unequiv-

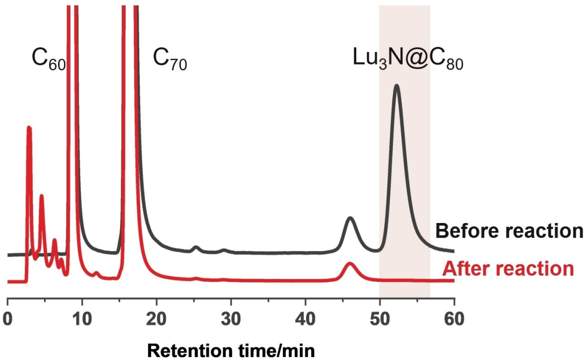

Figure 7. HPLC traces (5-PBB, toluene, 2 ml/min) of the mixture of C_{60}, C_{70} and $Lu_3N@C_{80}$ before (black) and after (red) reaction with **1b** and $Pb(OAc)_4$. The commercial C_{70} sample (certified as >97% purity) contained small amounts of higher fullerenes (C_{76}, C_{78}, C_{84}, etc.) which are visible at the current level of HPLC attenuation.

ocally showed that $Lu_3N@C_{80}$ reacts faster than empty fullerenes under the same conditions, consistent with the free-energy profile at room temperature (Figure S32), which also aligns with the intention of the IEDDA reaction design.

The unusual reactivity is rationalized by the lower Gibbs free energy barrier of $M_3N@C_{80}$ (Figure 6a, b) compared to that of C_{60} (18.2 kcal mol^{-1}) at 80 °C (Figure S33). This is also supported by the analysis of FMOs, where the gap between the HOMO of the EMF and the LUMO of the diimines (Figure S34) is much smaller than the counterpart for C_{60} (Figure 1a, Figure S35, 36 and Table S15).

Thermal Reversibility

In addition to the high reactivity, we also observed unusual reversibility in the new IEDDA reaction on EMFs. Although thermally reversible reactions have been reported for empty fullerenes,[53–55] in the case of EMFs, reverse reactions often require the addition of new reagents to run a different operation.[56,57] In this IEDDA reaction, however, complete reversibility was discovered during a heating experiment for the adduct **2b**, which was originally intended to probe any possible thermal isomerization between [5,6]- and [6,6]- regioisomers.[27,28] In the thermal test, toluene solution of adduct **2b** was heated at 100 °C for 1 h. There was no isomerization observed, instead, **2b** fully converted back to pristine $Lu_3N@C_{80}$ (Figure 8). The result suggests that the IEDDA reaction on $M_3N@C_{80}$ could be easily reversed by heating, and such reversibility was not observed in the reactions on C_{60} or C_{70}.

To shed light on the experimental findings, the activation energy barriers for the retro-cycloaddition of C_{60} and $Lu_3N@C_{80}$ were studied at 100 °C (Figure S37). The backward barrier, i.e., the Gibbs free energy difference between the adduct and the transition state, is 11.1 kcal mol^{-1} higher for the empty fullerene than for $Lu_3N@C_{80}$ (12.5 kcal mol^{-1} in the case of $Sc_3N@C_{80}$), consistent with the reversibility observed in experiments. The thermal retro-cycloaddition is insignificant in the formation of the **2a** and **3a** with excess of small-molecule reactants, as **2b** and **3b**, which are formed at room temperature, only have slightly higher yields.

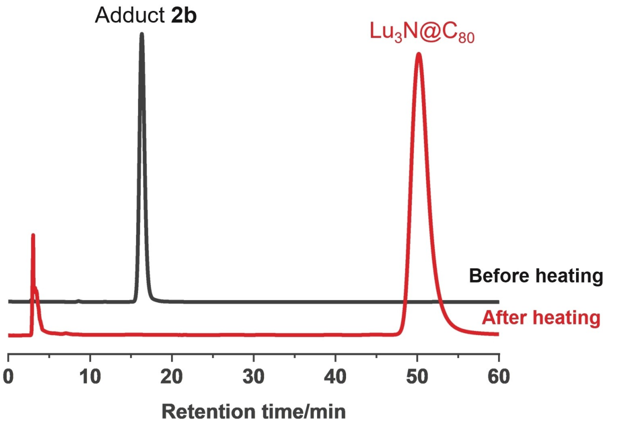

Figure 8. HPLC traces (5-PBB, toluene, 2 ml/min) of **2b** solution before (black) and after (red) heating at 100 °C.

The reversibility is an important trait that could lead to new applications. For example, it is conceivable to fabricate devices using solution-processable IEDDA derivatives and then thermally reverse the cycloaddition to regain the pristine EMFs for better semiconducting properties. Additionally, the IEDDA reaction could be used as an efficient chemical separation approach, as detailed below.

Chemical Separation of EMFs from Soot

In the production of EMFs, the soluble content in the soot is typically a complex mixture of fullerenes, predominantly containing C_{60}, C_{70} and higher fullerenes (98–99 %),[58] and only a small amount of EMFs. The isolation and purification of EMFs typically require solvent- and time-consuming chromatographic procedures, which are prohibitive for large-scale synthesis.[59]

In light of this, several chemical separation methods based on organic reactions have been developed, such as the functionalized resin approach[60] and the stir and filter approach (SAFA).[61] In these methods, the inherently inert nature of EMFs is exploited, whereby the empty fullerenes react with the functionalized immobile phase (e.g., resin or silica), while the unreacted EMFs remain in solution.

The most successful reaction used in such chemical separation methods is the more common "normal" electron demand DA reaction, which has excellent selectivity towards empty fullerenes over EMFs. A significant limitation of DA reaction-based separation, however, is the large amount of diene-functionalized silica or resin required, as it needs to remove ~99 % of the components in the mixture to isolate the remaining 1 %. Additionally, due to limited processing efficiency of the retro-addition, it is not economical to regenerate the reacted empty fullerenes from the immobile phase. Overall, although better than chromatography, current chemical separations are still not cost-effective and environmentally friendly. Using the IEDDA instead of the "normal" DA reaction fundamentally changes the chemical separation process, allowing for the selective reaction with small amounts of desired species (i.e., EMFs), isolating the product by solubility, and regenerating the material through the retro-reaction.

The Sc-containing soot extracts generated from real EMF synthesis, and a $Lu_3N@C_{80}$-containing fullerene mixture, both consisting of mostly empty fullerene (Figure 9a, S38a), were used to demonstrate the approach (Figure 9, S38). The electric-arc synthesis of Sc metallofullerene soot has been previously described in seminal works.[17,62,63] To treat the Sc soot, small amounts of **1b** and $Pb(OAc)_4$ were added to the soot extract, and the process was monitored by HPLC. The peak of $Sc_3N@C_{80}$ decreased dramatically after reacting at room temperature for 30 mins (Figure 9b). The formed cycloadduct **3b** is soluble in common non-aromatic solvents such as methylene chloride and chloroform and thereby separated from fullerenes (which don't dissolve) in large-scale. In our small-scale lab setup, **3b** was separated by

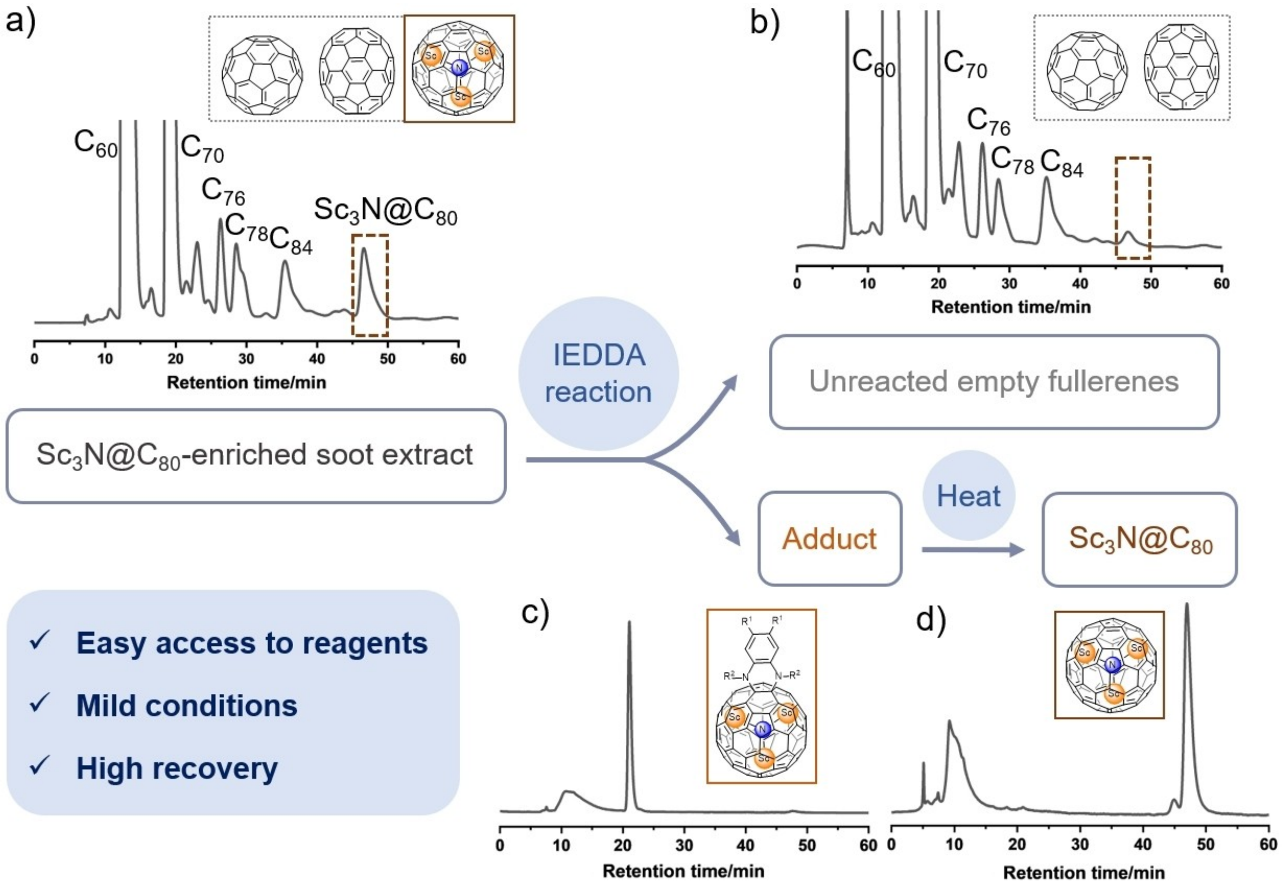

Figure 9. Flow chart of separation of $Sc_3N@C_{80}$ from soot extract along with HPLC traces (5-PYE, toluene, 2 ml/min) of every step: a) Soot extract generated from a Sc EMF synthesis, containing $Sc_3N@C_{80}$ as the main EMF component; b) Unreacted mixture; c) Isolated cycloadduct(s); d) Reaction mixture of the retro-cycloaddition, regenerating $Sc_3N@C_{80}$.

flash chromatography (Figure 9c). Finally, the cycloadduct **3b** was thermally converted back to pristine $Sc_3N@C_{80}$ (Figure 9d). An artificial mixture containing $Lu_3N@C_{80}$ (8.0 mg) C_{60} (120 mg) and C_{70} (70 mg) was used to provide quantitative insight for this procedure, and we were able to achieve 94 % recovery (7.5 mg) of the $Lu_3N@C_{80}$ (Figure S39).

With the IEDDA reaction-based chemical separation approach, the usage of reagents is substantially reduced compared to other methods because it is the $M_3N@C_{80}$ that reacts, rather than the empty fullerenes. The only precedent that utilized a reaction where EMFs have higher reactivity is the Lewis acid approach,[64] but even that process used a large excess of Lewis acids, and the selectivity required careful engineering based on types of fullerenes, Lewis acids, concentrations and reaction time, because the selectivity is not as clear-cut as the IEDDA reaction. In our work, about 94 % recovery of $M_3N@C_{80}$ can be achieved due to the complete retro-addition. Meanwhile, all the empty fullerenes are recycled as they remain pristine throughout the process. Ultimately, the IEDDA reaction provides a conceptually new organic chemistry-based method for separating EMFs with high efficiency.

Conclusion

In summary, we report a new IEDDA reaction on $M_3N@I_h$-C_{80} (M = Lu, Sc), resulting in [5,6]-closed [4+2] cycloadducts that are isolated and characterized by HPLC, MS, UV/Vis, NMR, and X-ray crystallography, in combination with DFT computations. In this reaction, EMFs exhibit higher reactivity compared to empty fullerenes due to the inverse electron demand. Moreover, a complete reverse reaction can be achieved upon thermal treatment. The distinctive reactivity and reversibility of the IEDDA reaction enable a new concept in the chemical separation methodology for EMFs, where the desired EMFs that typically “remain last” in traditional chemical separation methods “react first” and are regenerated by retro-additions. The new chemistry and processing approach provide a key step towards the application of EMFs in energy materials, electronic devices, and biomedicines.

Acknowledgements

J.Z. thanks the US National Science Foundation (NSF) for the CAREER Award CHE-2238629. J.M.P. and A.R.-F.

thank the Spanish Ministry of Science & Innovation (grant PID2023-149905NB-I00), the Generalitat de Catalunya (grant 2021 SGR 00110) and the URV for support. S.S. thanks the NSF for grant CHE-1465173 and CHE-2247272. We thank the NSF for the Major Research Instrumentation (MRI) program grant CHE-2117792 for purchase of the X-ray diffractometer used in this study. We also thank Drs. Jean Baum and Seho Kim for the assistance in high-field NMR acquisitions and Dr. Maria Besora for insightful discussions on the reaction mechanisms.

Conflict of Interest

The authors declare no conflict of interest.

Data Availability Statement

The data that support the findings of this study are available in the supplementary material of this article.

Keywords: endohedral fullerenes · cycloaddition · density functional calculations · chemical separation · crystallography

---

[1] A. A. Popov, S. Yang, L. Dunsch, *Chem. Rev.* **2013**, *113*, 5989–6113.
[2] X. Lu, L. Feng, T. Akasaka, S. Nagase, *Chem. Soc. Rev.* **2012**, *41*, 7723–7760.
[3] W. Shen, L. Bao, X. Lu, *Chin. J. Chem.* **2022**, *40*, 275–284.
[4] W. Cai, M. Zhang, L. Echegoyen, X. Lu, *Fundamental Research*, https://doi.org/10.1016/j.fmre.2023.12.004.
[5] T. Li, H. C. Dorn, *Small* **2017**, *13*, 1603152.
[6] T. Wang, C. Wang, *Small* **2019**, *15*, 1901522.
[7] W. P. Kopcha, R. Biswas, Y. Sun, S.-T. D. Chueng, H. C. Dorn, J. Zhang, *Chem. Commun.* **2023**, *59*, 13551–13561.
[8] F. Liu, D. S. Krylov, L. Spree, S. M. Avdoshenko, N. A. Samoylova, M. Rosenkranz, A. Kostanyan, T. Greber, A. U. B. Wolter, B. Büchner, A. A. Popov, *Nat. Commun.* **2017**, *8*, 16098.
[9] G. Velkos, D. S. Krylov, K. Kirkpatrick, L. Spree, V. Dubrovin, B. Büchner, S. M. Avdoshenko, V. Bezmelnitsyn, S. Davis, P. Faust, J. Duchamp, H. C. Dorn, A. A. Popov, *Angew. Chem. Int. Ed.* **2019**, *58*, 5891–5896.
[10] L. Spree, A. A. Popov, *Dalton Trans.* **2019**, *48*, 2861–2871.
[11] W. Li, C. Wang, T. Wang, *Chem. Commun.* **2021**, *57*, 10317–10326.
[12] Z. Hu, S. Yang, *Chem. Soc. Rev.* **2024**, *53*, 2863–2897.
[13] Z. Hu, B.-W. Dong, Z. Liu, J.-J. Liu, J. Su, C. Yu, J. Xiong, D.-E. Shi, Y. Wang, B.-W. Wang, A. Ardavan, Z. Shi, S.-D. Jiang, S. Gao, *J. Am. Chem. Soc.* **2018**, *140*, 1123–1130.
[14] A. Jaroš, E. F. Bonab, M. Straka, C. Foroutan-Nejad, *J. Am. Chem. Soc.* **2019**, *141*, 19644–19654.
[15] J. Li, S. Hou, Y. R. Yao, C. Zhang, Q. Wu, H. C. Wang, H. Zhang, X. Liu, C. Tang, M. Wei, W. Xu, Y. Wang, J. Zheng, Z. Pan, L. Kang, J. Liu, J. Shi, Y. Yang, C. J. Lambert, S. Y. Xie, W. Hong, *Nat. Mater.* **2022**, *21*, 917–923.
[16] J. Qiu, L. Abella, X. Du, Z. Cao, Z. He, Q. Meng, Y. Yan, J. M. Poblet, L. Sun, A. Rodríguez-Fortea, N. Chen, *J. Am. Chem. Soc.* **2024**, *146*, 24310–24319.
[17] S. Stevenson, G. Rice, T. Glass, K. Harich, F. Cromer, M. R. Jordan, J. Craft, E. Hadju, R. Bible, M. M. Olmstead, K. Maitra, A. J. Fisher, A. L. Balch, H. C. Dorn, *Nature* **1999**, *401*, 55–57.
[18] J. Zhang, S. Stevenson, H. C. Dorn, *Acc. Chem. Res.* **2013**, *46*, 1548–1557.
[19] T. Wang, C. Wang, *Acc. Chem. Res.* **2014**, *47*, 450–458.
[20] Y. Iiduka, O. Ikenaga, A. Sakuraba, T. Wakahara, T. Tsuchiya, Y. Maeda, T. Nakahodo, T. Akasaka, M. Kako, N. Mizorogi, S. Nagase, *J. Am. Chem. Soc.* **2005**, *127*, 9956–9957.
[21] T. Wakahara, Y. Iiduka, O. Ikenaga, T. Nakahodo, A. Sakuraba, T. Tsuchiya, Y. Maeda, M. Kako, T. Akasaka, K. Yoza, E. Horn, N. Mizorogi, S. Nagase, *J. Am. Chem. Soc.* **2006**, *128*, 9919–9925.
[22] M. Yamada, T. Abe, C. Saito, T. Yamazaki, S. Sato, N. Mizorogi, Z. Slanina, F. Uhlík, M. Suzuki, Y. Maeda, Y. Lian, X. Lu, M. M. Olmstead, A. L. Balch, S. Nagase, T. Akasaka, *Chem. Eur. J.* **2017**, *23*, 6552–6561.
[23] E. B. Iezzi, J. C. Duchamp, K. Harich, T. E. Glass, H. M. Lee, M. M. Olmstead, A. L. Balch, H. C. Dorn, *J. Am. Chem. Soc.* **2002**, *124*, 524–525.
[24] H. M. Lee, M. M. Olmstead, E. Iezzi, J. C. Duchamp, H. C. Dorn, A. L. Balch, *J. Am. Chem. Soc.* **2002**, *124*, 3494–3495.
[25] S. Stevenson, R. R. Stephen, T. M. Amos, V. R. Cadorette, J. E. Reid, J. P. Phillips, *J. Am. Chem. Soc.* **2005**, *127*, 12776–12777.
[26] T. Cai, L. Xu, M. R. Anderson, Z. Ge, T. Zuo, X. Wang, M. M. Olmstead, A. L. Balch, H. W. Gibson, H. C. Dorn, *J. Am. Chem. Soc.* **2006**, *128*, 8581–8589.
[27] T. Cai, C. Slebodnick, L. Xu, K. Harich, T. E. Glass, C. Chancellor, J. C. Fettinger, M. M. Olmstead, A. L. Balch, H. W. Gibson, H. C. Dorn, *J. Am. Chem. Soc.* **2006**, *128*, 6486–6492.
[28] S. Aroua, Y. Yamakoshi, *J. Am. Chem. Soc.* **2012**, *134*, 20242–20245.
[29] C. M. Cardona, A. Kitaygorodskiy, L. Echegoyen, *J. Am. Chem. Soc.* **2005**, *127*, 10448–10453.
[30] O. Lukoyanova, C. M. Cardona, J. Rivera, L. Z. Lugo-Morales, C. J. Chancellor, M. M. Olmstead, A. Rodríguez-Fortea, J. M. Poblet, A. L. Balch, L. Echegoyen, *J. Am. Chem. Soc.* **2007**, *129*, 10423–10430.
[31] C. Shu, T. Cai, L. Xu, T. Zuo, J. Reid, K. Harich, H. C. Dorn, H. W. Gibson, *J. Am. Chem. Soc.* **2007**, *129*, 15710–15717.
[32] C. Shu, C. Slebodnick, L. Xu, H. Champion, T. Fuhrer, T. Cai, J. E. Reid, W. Fu, K. Harich, H. C. Dorn, H. W. Gibson, *J. Am. Chem. Soc.* **2008**, *130*, 17755–17760.
[33] A.-C. Knall, C. Slugovc, *Chem. Soc. Rev.* **2013**, *42*, 5131–5142.
[34] Z. M. Png, H. Zeng, Q. Ye, J. Xu, *Chem. Asian J.* **2017**, *12*, 2142–2159.
[35] Y. Sun, C. Qian, T. J. Emge, Y. Li, W. P. Kopcha, L. Wang, J. Zhang, *Org. Lett.* **2022**, *24*, 6417–6422.
[36] H. Kawakami, H. Okada, Y. Matsuo, *Org. Lett.* **2013**, *15*, 4466–4469.
[37] H. Ueno, H. Kawakami, K. Nakagawa, H. Okada, N. Ikuma, S. Aoyagi, K. Kokubo, Y. Matsuo, T. Oshima, *J. Am. Chem. Soc.* **2014**, *136*, 11162–11167.
[38] Y. Matsuo, H. Okada, M. Maruyama, H. Sato, H. Tobita, Y. Ono, K. Omote, K. Kawachi, Y. Kasama, *Org. Lett.* **2012**, *14*, 3784–3787.
[39] H. Ueno, Y. Yamazaki, H. Okada, F. Misaizu, K. Kokubo, H. Sakurai, *Beilstein J. Org. Chem.* **2024**, *20*, 653–660.
[40] Y. Rubin, S. Khan, D. I. Freedberg, C. Yeretzian, *J. Am. Chem. Soc.* **1993**, *115*, 344–345.
[41] A. Chikama, H. Fueno, H. Fujimoto, *J. Phys. Chem.* **1995**, *99*, 8541–8549.
[42] X.-F. Gao, C.-X. Cui, Y.-J. Liu, *J. Phys. Org. Chem.* **2012**, *25*, 850–855.
[43] C. Niu, Z. Liu, M. Chen, S. Yang, G.-W. Wang, *Org. Lett.* **2022**, *24*, 3493–3498.

[44] Z. Liu, Z.-C. Yin, W.-Q. Lu, D.-B. Zhou, G.-W. Wang, *Chem. Commun.* **2021**, *57*, 13389–13392.
[45] A. Dhamija, A. Gunnam, X. Yu, H. Lee, I.-C. Hwang, Y. Ho Ko, K. Kim, *Angew. Chem. Int. Ed.* **2022**, *61*, e202209326.
[46] D. Wang, H. Yu, S. Sun, F. Zhong, *Org. Lett.* **2020**, *22*, 2425–2430.
[47] S. Aroua, M. Garcia-Borràs, S. Osuna, Y. Yamakoshi, *Chem. Eur. J.* **2014**, *20*, 14032–14039.
[48] F.-F. Li, J. R. Pinzón, B. Q. Mercado, M. M. Olmstead, A. L. Balch, L. Echegoyen, *J. Am. Chem. Soc.* **2011**, *133*, 1563–1571.
[49] Y. Maeda, M. Kimura, C. Ueda, M. Yamada, T. Kikuchi, M. Suzuki, W.-W. Wang, N. Mizorogi, N. Karousis, N. Tagmatarchis, T. Hasegawa, M. M. Olmstead, A. L. Balch, S. Nagase, T. Akasaka, *Chem. Commun.* **2014**, *50*, 12552–12555.
[50] M. Kako, T. Sugiura, K. Miyabe, M. Yasui, M. Yamada, Y. Maeda, J.-D. Guo, S. Nagase, T. Akasaka, *Chem. Asian J.* **2017**, *12*, 1391–1399.
[51] S. Sato, Y. Maeda, J.-D. Guo, M. Yamada, N. Mizorogi, S. Nagase, T. Akasaka, *J. Am. Chem. Soc.* **2013**, *135*, 5582–5587.
[52] K. Sato, M. Kako, M. Suzuki, N. Mizorogi, T. Tsuchiya, M. M. Olmstead, A. L. Balch, T. Akasaka, S. Nagase, *J. Am. Chem. Soc.* **2012**, *134*, 16033–16039.
[53] I. Lamparth, C. Maichle–Mössmer, A. Hirsch, *Angew. Chem. Int. Ed.* **1995**, *34*, 1607–1609.
[54] B. Nie, V. M. Rotello, *J. Org. Chem.* **1996**, *61*, 1870–1871.
[55] B. Kräutler, T. Müller, A. Duarte-Ruiz, *Chem. Eur. J.* **2001**, *7*, 3223–3235.
[56] N. Martín, M. Altable, S. Filippone, A. Martín-Domenech, L. Echegoyen, C. M. Cardona, *Angew. Chem. Int. Ed.* **2006**, *45*, 110–114.
[57] B. Wu, T. Wang, Z. Zhang, Y. Feng, L. Gan, L. Jiang, C. Wang, *Chem. Commun.* **2013**, *49*, 10489–10491.
[58] W. Krätschmer, L. D. Lamb, K. Fostiropoulos, D. R. Huffman, *Nature* **1990**, *347*, 354–358.
[59] K. Kikuchi, N. Nakahara, M. Honda, S. Suzuki, K. Saito, H. Shiromaru, K. Yamauchi, I. Ikemoto, T. Kuramochi, S. Hino, Y. Achiba, *Chem. Lett.* **1991**, *20*, 1607–1610.
[60] Z. Ge, J. C. Duchamp, T. Cai, H. W. Gibson, H. C. Dorn, *J. Am. Chem. Soc.* **2005**, *127*, 16292–16298.
[61] S. Stevenson, K. Harich, H. Yu, R. R. Stephen, D. Heaps, C. Coumbe, J. P. Phillips, *J. Am. Chem. Soc.* **2006**, *128*, 8829–8835.
[62] S. Stevenson, M. A. Mackey, M. C. Thompson, H. L. Coumbe, P. K. Madasu, C. E. Coumbe, J. P. Phillips, *Chem. Commun.* **2007**, 4263–4265.
[63] S. Stevenson, H. M. Lee, M. M. Olmstead, C. Kozikowski, P. Stevenson, A. L. Balch, *Chem. Eur. J.* **2002**, *8*, 4528–4535.
[64] S. Stevenson, M. A. Mackey, J. E. Pickens, M. A. Stuart, B. S. Confait, J. P. Phillips, *Inorg. Chem.* **2009**, *48*, 11685–11690.

Manuscript received: December 17, 2024
Accepted manuscript online: February 9, 2025
Version of record online: ■■, ■■

Research Article

Endohedral Fullerenes

Y. Sun, L. Abella, T. J. Emge, S. Zhu, Y. Li, I. Ferraro, A. Li, S. Stevenson, J. M. Poblet, A. Rodríguez-Fortea,* J. Zhang* **e202424776**

Inverse Electron Demand Diels–Alder Reaction on $M_3N@C_{80}$ (M = Lu, Sc): Reactivity and Reversibility Enable Chemical Separation of Metallofullerenes

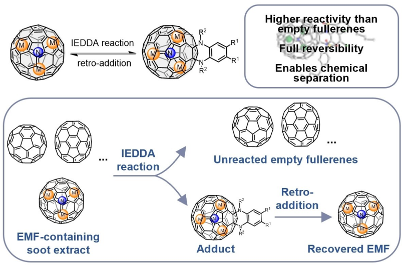

An inverse electron demand Diels–Alder (IEDDA) reaction on $M_3N@I_h\text{-}C_{80}$ (M = Lu, Sc) has been utilized to yield [5,6]-closed [4 + 2] cycloadducts that were fully characterized (HPLC, MS, UV/Vis and NMR spectroscopy, X-ray crystallography, and DFT calculations). The unique reactivity and thermal reversibility of endohedral metallofullerenes enable an efficient separation strategy, thereby advancing scalable synthesis for future applications.